Two-dimensional scattering of a plane wave from a periodic array of dielectric cylinders with arbitrary shape

Mitsuhiro Yokota[1,*] and Maurice Sesay[1]

[1]Department of Electrical and Electronic Engineering, University of Miyazaki, Miyazaki 889-2192, Japan

A two-dimensional scattering of a plane wave from a periodic array of dielectric cylinders with arbitrary shape using multigrid-moment method is examined in this paper. The scattered field is expressed in terms of the integral form by an infinite summation of the surface integral over the cross section of the reference cylinder. The integral form is converted into the matrix equation by using moment method. The integration in the elements of the matrix equation is evaluated by the lattice sums technique in order to obtain precise solution. The multigrid method is applied to the matrix equation to improve the CPU time. As numerical results, the CPU time and residual norm are examined for a given number of iteration and cycle index. After that, the effects of shape and material of the periodic structure on the power reflection coefficient of the fundamental Floquet mode are shown. The results also indicate the effect of changing the relative permittivity of the dielectric coated body and the reflection coefficient.

OCIS codes: 050.2770, 050.1755, 290.5850

*Corresponding author: m.yokota@m.ieice.org

1. Introduction

Periodic structures that have very interesting and useful properties have been used as the frequency selective filters and polarization filters [1]. Recently, the interest in photonic crystals as the periodic structures has increased, since there exists the specific frequency selective properties [2, 3]. These structures have many applications in the design of antennas and waveguide for bandwidth enhancement or dual-band applications. The frequency response of the array is characterized by the scattering properties of the individual objects and the multiple scattering due to the periodic arrangement of scatterers. When the shape of the scatterer is the circular cylinder or sphere, the eigen-function expansion method can be used in order to examine the scattering properties. On the other hand, the numerical technique such as the finite element method [4], the differential method [5], the time domain methods [6, 7], etc are used for the arbitrary shape and the complex structures. Moment Method (MoM) [8] has been applied to various problems in the electromagnetic and optics fields and is one of the useful numerical methods to obtain the good accuracy.

When the size of the matrix becomes large, it is well known that the load of CPU and/or a computer memory increases. In this case, the fast solver for the matrix equation is needed. Multigrid method [9, 10, 11] developed by Brandt [12] is known as one of fast solvers. This method attempts to obtain a converging solution at high speed by means of iterative calculations between several computation grids with different sizes. It was shown that Multigrid Method combined with MoM improves the computational time needed to carry out the numerical analysis [13].

In this paper, the multigrid-moment method is applied to a two-dimensional scattering

of a plane wave from a periodic array of dielectric cylinders with arbitrary shape. The scattered field is obtained by the volume equivalent theorem [14]. The integral form is converted into the matrix equation by MoM. The Multigrid method is applied to this matrix equation to solve as fast as possible. In addition to this, the dense matrix coefficient expressed in the periodic Green's function of arbitrary high order can be simplified to an integral form of elementary functions. These elementary functions constitute the lattice sums expression used in [15] because this expression only depends on the geometrical parameter of the structure. Using the lattice sums technique [15], the computational time for the numerical evaluation decreases drastically. In the multigrid scheme, three multigrid levels are taken into consideration and GMRES (Generalized Minimum Residual) method [16] is applied as the relaxation method in all of the grid levels. As numerical results, the effect of shape and material of the periodic structure on the power reflection coefficient are shown. We also show the effect of changing the relative permittivity of the composite dielectric body and the reflection coefficient for the fundamental reflection coefficient of the periodic structure.

2. Formulation

Consider the scattering from a periodic array of dielectric cylinders with arbitrary shape along the x-direction with periodicity d as shown in Fig. 1. It is assumed that the incident plane wave E_i is polarized along the z-axis, which corresponds to an E-polarized wave. In this case, the scattered field at any point of the structure is obtained using the result of scattering by one cylinder [14], and Floquet's theorem. The total electric field $E(\mathbf{r})$ is the

superposition of the incident field $E_i(\mathbf{r})$ and scattered field $E_s(\mathbf{r})$ as follows:

$$E(\mathbf{r}) = E_i(\mathbf{r}) - j\frac{k^2}{4}\sum_{l=-\infty}^{\infty}\int_{s_0} H_0^{(2)}(k\rho_l)E(\mathbf{r}_0)\exp(-jk_x ld)(\varepsilon_r - 1)ds_0 \tag{1}$$

where $k_x = -k\sin\theta_i$, k is the wavenumber of free space, θ_i is the incident angle with respect to the y-axis. The integration is performed on the reference cylinder. H_0^2 is the zeroth-order Hankel function of the second kind. $E(\mathbf{r}_0)$ is unknown total electric field and ρ_l is the distance between the observation point $\mathbf{r}$ and source point $\mathbf{r}_0$ of the reference cylinder. To obtain the form of the matrix equations for Eq. (1) by MoM, the pulse function as the basis function is used. The reference cylinder is divided in N number of cells and the total electric field and the relative permittivity is assumed to be constant on each cell. The form of the matrix equation is as follows:

$$\sum_{n=1}^{N} C_{mn}E_n = E_m^i \qquad m = 1, \cdots, N \tag{2}$$

The expression of the coefficient C_{mn} is given as follows

$$C_{mn} = j\frac{\pi}{2}[\varepsilon_r(n) - 1]ka_n J_1(ka_n)\sum_{l=-\infty}^{\infty}\exp(-jk_x ld)H_0^{(2)}(k\rho_{mn}^l) \quad (m \neq n) \tag{3}$$

and

$$C_{nn} = 1 + j\frac{\pi}{2}[\varepsilon_{r0}(n) - 1]\left[\left\{ka_n H_1^{(2)}(ka_n) - \frac{2j}{\pi}\right\} + ka_n J_1(ka_n)\sum_{l=-\infty,\, l\neq 0}^{\infty}\exp(-jk_x ld)H_0^{(2)}(k\rho_{nn}^l)\right] \quad (m = n) \tag{4}$$

where a_n is the radius of the equivalent circular cell with the same cross-sectional area. The integration on the reference cylinder is approximated by Richmond approximation [14]. The distance ρ_{mn}^l is defined as $\sqrt{(x_m - ld)^2 + y_m^2)}$ and x_m, y_m are the centers of the mth cell with the location of the reference cylinder.

The scattered field at observation point $\mathbf{r}$ is obtained by using the total electric fields in the cylinder as follows:

$$E_s(x,y) = -\sum_{n=1}^{N} C_{mn} E_n \tag{5}$$

where the coefficient C_{mn} is given by Eqs. (3) and (4) with $x_m = x$ and $y_n = y$.

The evaluation of the infinite sum of Hankel functions multiplied by trigonometric angular dependencies in Eqs. (3) and (4) is the most time consuming part in the scattering problem of periodic structures. In order to obtain the summation efficiently with less computational time, two numerical techniques are applied. One is lattice sums technique [15] and another is multigrid method [11].

A H-polarized wave whose magnetic wave is parallel to the cylindrical axis can be treated in the same procedure presented in this paper. For a H-polarized wave, the electric wave has two components. Since the equivalent current which is related to the electric waves is used in the formulation, the above procedure is applied to these two components, and then, the matrix equation for the electric waves can be obtained [14].

3. Lattice Sums Technique

The coefficient C_{mn} includes the following periodic Green's function.

$$\begin{aligned}\sum_{l=-\infty}^{\infty} &\exp(jkld\sin\theta_i) H_0^{(2)}(k\rho_{mn}^l) \\ &= \left[H_0^2(k\rho) + S_0(kd,\theta_i) J_0(k\rho) + 2\sum_{p=1}^{\infty} S_p(kd,\theta_i) J_p(k\rho)\cos(p\phi)\right]\end{aligned} \tag{6}$$

where

$$S_p(kd,\theta_i) = \sum_{l=1}^{\infty} H_p^{(2)}(lkd)\exp\left(jlkd\sin\theta_i\right) + \sum_{l=1}^{\infty}(-1)^p H_p^{(2)}(lkd)\exp\left(-jlkd\sin\theta_i\right) \tag{7}$$

and J_n is Bessel function of the nth order and $\rho = \sqrt{x_m^2 + y_m^2}$, and $\phi = \cos^{-1}(x_m/\rho)$. By using the integral representation of Hankel function, the first term of Eq. (7) is written as follows [15]:

$$\sum_{l=1}^{\infty} H_p^{(2)}(lkd) \exp(jlkd \sin\theta_i)$$
$$= (-1)^p \exp\{j(\pi/4 + kd \sin\theta_i)\} \frac{\sqrt{2}}{\pi} \int_0^a [G_p(\tau) + G_p(-\tau)] \cdot F(\tau; kd, \sin\theta_i) dt \quad (8)$$

where

$$G_p = (t - j\sqrt{1-t^2})^p \quad (9)$$

$$F(\tau; kd, \sin\theta_i) = \frac{e^{-jkd\sqrt{1-t^2}}}{\sqrt{1-t^2}[1 - e^{-jkd(\sqrt{1-t^2} - \sin\theta_i)}]} \quad (10)$$

and p denotes the number of cylindrical harmonics and a the integration limit. p is evaluated from the Bessel function of the p-order $J_p(k\rho)$ and the integration limit was attained using numerical integration.

4. Multigrid Method

Multigrid method attempts to obtain a converging solution at high speed by means of iterative calculations between several computation grids with different sizes. The outline of two levels V-shape multigrid scheme is as follows [11]:

1. Initial guess is assumed at the fine grid. Then GMRES method is applied to the matrix equation on the fine grid until a convergence is attained. The residual at the fine grid is then computed.

2. The residual at the fine grid is then restricted to the course grid using the the weighting average operator [11]. The relaxation scheme such as GMRES method is applied to

the correction matrix equation on the course grid and the guess is corrected for one iteration step.

3. The corrected term at the course grid is interpolated to the fine grid using the bilinear interpolation operator [11] and the guess is modified. GMRES method is applied to the matrix equation using the modified guess as initial value to obtain a new approximate solution.

When the above V-shape cycle multigrid scheme is applied recursively, a W-cycle multigrid scheme can be formed as shown in Fig. 2.

5. Numerical Results

As the numerical results, an E-polarised wave incidence is considered. The reflection properties from a periodic array of dielectric cylinders is firstly examined in order to verity the validity of the method in this paper. The CPU time, residual norm and effect of initial values on the convergence speed are examined for the case of the periodic circular cylinders.

Figure 3 indicates the normalized residual norm and CPU time for various cycle indices γ of W cycles for the periodic circular cylinder when $a/\lambda = 0.3, d/\lambda = 0.999, \varepsilon_r = 2.0$ and The number of unknowns $N = 8100$. The structure of the multigrid is three level scheme and the matrix equation on the finest grid is solved under the condition that the normalized residual norm is less than 10^{-5}. When the cycle index increases, the residual norm decreases and the CPU time increases. In the same case, GMRES method with the condition that the normalized residual norm is less than 10^{-7} is applied and the CPU time is 29.1 sec. It is found from Fig. 3 that the CPU time for the multigrid method is 17.1 sec for the number

of multigrid cycles 3 and $\gamma = 5$ or 6. Then, the multigrid method is useful and suitable for the periodic structure.

The initial value for the multigrid would affects the convergence of the residual norm. The convergence tendency is similar to the results of scattering by two dielectric cylinders [13]. The normalised residual norm and CPU time for the number of multigrid cycles using the proposed scheme in Fig. 4 is indicated in Fig. 5. For the residual norm less than10^{-7}, the number of multigrid cycles and CPU is 2 and 5.91 sec, respectively. It is found that the CPU time is improved and the proposed scheme is suitable for the periodic structure.

In what follows, we examine the reflection properties from the periodic array of the dielectric cylinders using the scheme in Fig. 4. The scattered field $E_s(x, y)$ is obtained using the integral representation of Hankel function as follows:

$$E_s = \frac{-j}{2} \sum_{n=1}^{N} E_n \, [\varepsilon_{r0}(n) - 1] k a_n J_1(k a_n) \times \sum_{l=-\infty}^{\infty} \frac{1}{\kappa(k_{x,l})} \exp[+jk_{x,l}x_n^0 + j\kappa(k_{x,l})y_n^0] \exp[-jk_{x,l}x - j\kappa(k_{x,l})y] \tag{11}$$

where

$$k_{x,l} = k_x + l\frac{2\pi}{d} \tag{12}$$

$$\kappa(k_{x,l}) = \sqrt{k^2 - k_{x,l}^2}\,, \qquad \mathrm{Im}(\kappa(k_{x,l})) \leq 0 \tag{13}$$

After the following relation is used,

$$\sum_{l=-\infty}^{\infty} \exp[-jk_x ld + j\xi ld] = \frac{2\pi}{d} \sum_{l=-\infty}^{\infty} \delta\left(\xi - k_x - l\frac{2\pi}{d}\right) \tag{14}$$

the reflection coefficient of lth order of the space harmonics is obtained as follows:

$$R_l = \frac{-j}{2} \sum_{n=1}^{N} E_n \, [\varepsilon_{r0}(n) - 1] k a_n J_1(k a_n) \frac{1}{\kappa(k_{x,l})} \exp\left[+jk_{x,l}x_n^0 + j\kappa(k_{x,l})y_n^0\right] \tag{15}$$

We discuss the power reflection coefficient from a periodic array of the circular cylinders for the fundamental mode. The numerical calculation depends on the parameters and the geometry. In this paper, the truncated number for $S_p(kd, \theta_i)$ in Eq. (6) is set to be $|p| = 13$ for the conservation energy error of the Bessel function taken to be 10^{-5}. The numerical integration limit in Eq. (8) is chosen as $a = 8$ when the error is less than 10^{-3}. The number of unknowns for the dielectric cylinder is set to be $N = 3600$.

We first of all confirm the presented method by comparing the computational time and the power reflection coefficient for a periodic array of circular cylinders with the radius $0.3d$ [17]. Figure 6 shows the power reflection coefficient $|R_0|^2$ for the effect of changing the permittivity for the circular cylinders of radius $0.3d$. The accuracy of using lattice sums together with multigrid-moment method is compared with the previous result and is confirmed the good agreement each other for $\varepsilon_r = 2.0$. It is shown from this figure that the peak of the power reflectance moves to the higher frequency and is controllable with the permittivity. Also, the side-band of the power reflectance reduces by decreasing the permittivity of the cylinder.

The power reflection coefficient $|R_0|^2$ for the circular cylinders that is coated with a circular shape dielectric material at various position within the cylinder is indicated in Fig. 7. The inner circular cylinder is allocated as that the outer one may be touched. The definition of the angle ϕ_{gr} is indicated in the inset. We experience a single resonance peak with a broader side-band reflectance profile when $\phi_{gr} = 0^\circ$. When $\phi_{gr} > 0^\circ$, it is found that two peaks are shifted toward a lower and higher d/λ values with reduced side-band reflectance. From this result, the inner cylinder affects the frequency that gives the peak of

the power reflectance.

Next, the reflection property from the elliptical cylinder coated with the circular body as shown in Fig. 8 is examined. The axis dimension, radius and relative permittivity of the cylinder and the coated body are given by (a, b, ε_{r1}) and (R_2, ε_{r2}), respectively. d_{12} is the distance between the centers of the coated circular body and the cylinder. e is the eccentricity defined as

$$b = a\sqrt{1 - e^2} \tag{16}$$

At first, we consider the scattering by the elliptical cylinder without the inner cylinder. Figure 9 shows the power reflection coefficient $|R_0|^2$ for various eccentricities of the elliptical cylinder. The eccentricity affects the resonance profile. Decreasing the eccentricity affects the shift of the resonance frequency to a lower value on to the point when $e = 0.5$. When $e < 0.5$, the difference of the reflection property is small because the shape has gradually tended to a circular shape.

Figure 10 shows the power reflection coefficients $|R_0|^2$ as a function of the normalised wavelength d/λ for various ε_{r2} of the elliptical cylinder that has eccentricity of 0.86 and $a = 0.3d$. A single resonance peak is noticeable but the side-band reflectance property is narrow for the case when $\varepsilon_{r2} = 1.5$ and broaden when ε_{r2} increases with a depictable lowering of the normalised resonance wavelength.

Figure 11 shows the power reflection coefficients $|R_0|^2$ as a function of the normalised wavelength d/λ where the elliptical cylinder of eccentricity 0.3 with $a = 0.3d$ and relative permittivity of 1.5 is coated with two circular dielectric cylinders with radius of $r_1 = 0.1d$. One of the body is coated at the center of the elliptical cylinder and the other at $0.2d$ from

the center of the elliptical cylinder. We observe two noticeable resonance peaks and there exists the frequency of $|R_0|^2 = 0$. The resonance peaks depict the multiple scattering effect between the elliptical cylinder and the coated circular cylinders. When ε_{r1} increases, the peaks are shifted toward lower d/λ values with broader side-band reflectance properties.

Figure 12 shows the total intensity contour map for $d = 0.902\lambda$, $\varepsilon_{r1} = 3.23$, $\varepsilon_{r2} = 1.5$, $R_1 = 0.1d$, $d_{12} = 0.2d$ with the eccentricity of the elliptical cylinder of 0.3 and $a = 0.3d$. As it is shown in Fig. 12, the total field intensity is very strong between the array on to the point $y < 0.5\lambda$ and stronger for $y > 0.5\lambda$ above each array cylinder. A propagating plane wave near the point $y = \lambda$, $y = 1.5\lambda$ and $y = 2\lambda$ is observed.

6. Conclusions

The scattering from a periodic array of dielectric cylinders with arbitrary shape has been analyzed by using both of lattice sums technique and multigrid-moment method. At first, the validity of the presented method has been examined from the CPU time and residual norm points of view. It can be shown the effect of not only the computational time but also the accuracy of the result. After that, the effect of the shape and material of the structure has been investigated. For the circular cylinder, the permittivity affects the frequency that gives the peaks of the maximum power reflection. Also, the periodic structure with coated dielectric material for both of the circular and elliptical cylinder affects the resonance properties of the structure. This phenomena has the possibility as a frequency selection device.

The layered periodic array of dielectric cylinders is also of significant importance for getting a better performance of optical grating structure. The presented method can be extended to the layered periodic array using reflection and transmission matrices. The scat-

tered wave is decomposed into the up-going and down-going waves. Applying the boundary condition on the artificial boundary of each layer leads to the relation of the reflection and transmission. The detailed examination is one of the future works. Also, the optimal parameter for the filter will be considered using the optimization algorithm from the practical point of view.

References

1. R. Petit, ed., *Electromagnetic Theory of Grating* (Springer-Verlag, 1980).
2. K. Sakoda, *Optical Properties of Photonic Crystals* (Springer, 2001).
3. K. Yasumoto, ed., *Electromagnetic Theory and Applications for Photonic Crystal* (Taylor &Francis, 2006).
4. G. Pelosi, A. Cocchi, and A. Monorchio, "A hybrid fem-based procedure for the scattering from photonic crystals illuminated by a Gaussian beam," IEEE Trans. Antennas and Propag. **48**, 973–980 (2000).
5. E. Popov and B. Bozhkov, "Differential method applied for photonic crystals," Appl. Opt. **39**, 4926–4933 (2000).
6. M. Koshiba, Y. Tsuji, and M. Hikari, "Time-domain beam propagation method and its application to photonic crystal circuits," J. Lightwave Technol. **18**, 102–110 (2000).
7. H. Ikuno and Y. Naka, *Finite-difference time-domain method applied to photonic crystals* in *Electromagnetic Theory and Applications for Photonic Crystal* ed. K. Yasumoto (Taylor & Francis, 2006), pp.401–444.
8. R. Harrington, *Field Computation by Moment Methods* (IEEE Press, 1993).
9. P. Wesseling, *An Introduction to Multigrid Methods* (John Wiley & Sons, 1992).
10. W. H. Press, S. A. Teukolsky, W. T. Vetterling, and B. P. Flannery, *Numerical Recipes in FORTRAN (2nd Edition)* (Cambridge University Press, 1992).
11. U. Trottenberg, C. Oosterlee, and A. Schüller, *Multigrid* (Academic Press, 2001).
12. A. Brandt, "Multi-level adaptive solutions to boundary-value problems," Math. Comput. **31**, 333–390 (1977).

13. M. Yokota and K. Aoyama, "Scattering of a Gaussian beam by dielectric cylinders with arbitrary shape using multigrid-moment method," Trans. IEICE **E90–C**, 258–264 (2007).

14. A. Ishimaru, *Electromagnetic Wave Propagation, Radiation, and Scattering* (Prentice Hall, 1991).

15. K. Yasumoto and K. Yoshitomi, "Efficient calculation of lattice sums for free-space periodic green's function," IEEE Trans. Antennas Propag. **47**, 1050–1055 (1999).

16. Y. Saad and M. H. Schultz, "GMRES: A generalized minimum residual algorithm for solving nonsymmetric linear systems," SIAM J. Sci. Stat. Comput. **7**, 856–869 (1986).

17. K. Kushta and K. Yasumoto, "Electromagnetic scattering from periodic arrays of two circular cylinders per unit cell," Progress In Electromagnetics Research **PIER 29**, 69–85 (2000).

List of Figure Captions

Fig. 1. Geometry of a periodic array of dielectric cylinders with arbitrary shape.

Fig. 2. Structure of W cycle with cycle index $\gamma = 3$ and three levels.

Fig. 3. Normalized residual norm and CPU time for several cycle indices. The number of unknowns 8100 and the matrix equation on the finest grid is solved under the condition that the normalized residual norm is less than 10^{-5}.

Fig. 4. Scheme for the improvement of the initial values for the multigrid.

Fig. 5. Normalized residual norm and CPU time for several cycle indices using the scheme indicated in Fig. 4.

Fig. 6. Power reflection coefficient $|R_0|^2$ of the fundamental space harmonics for several different relative permittivity as function of the normalized frequency d/λ; radius of circular cylinder is $0.3d$.

Fig. 7. Power reflection coefficient$|R_0|^2$ of the fundamental space harmonics for several different inclination angles Φ_{gr} as function of the normalized frequency d/λ; $\varepsilon_r = 2.25, \varepsilon_2 = 2.0, r_1 = 0.15d, r_2 = 0.3d$.

Fig. 8. Geometry of a periodic array of composite elliptical cylinders.

Fig. 9. Power reflection coefficient $|R_0|^2$ of the fundamental space harmonics for several different eccentricities as function of the normalized frequency d/λ; $a = 0.3d$ and $\varepsilon_2 = 2.0$.

Fig. 10. Power reflection coefficient $|R_0|^2$ of the fundamental space harmonics for several different relative permittivity as function of the normalized frequency d/λ; $a = 0.3d$ and eccentricity is 0.86.

Fig. 11. Power reflection coefficient$|R_0|^2$ of the fundamental space harmonics for the elliptical cylinder where two circular cylinders are contained as function of the normalized frequency d/λ; $a = 0.3$ and eccentricity is 0.3.

Fig. 12. Distribution of the total intensity contour distribution map; $d = 0.902\lambda$, $\varepsilon_{r1} = 3.23$, $R_1 = 0.1d$ and the eccentricity of the elliptical cylinder is 0.3 with $a = 0.3d$.

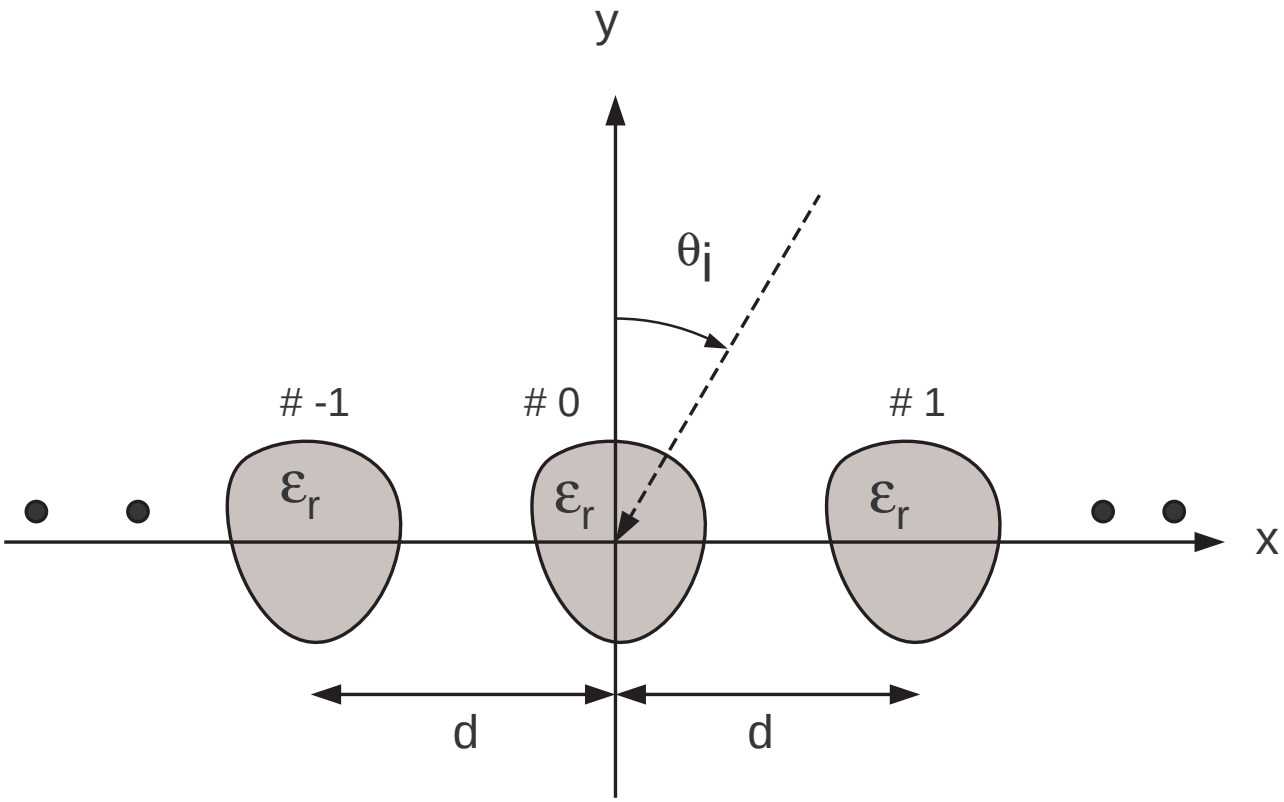

Fig. 1. Geometry of a periodic array of dielectric cylinders with arbitrary shape. Yokota_JOSAA_fig1.eps.

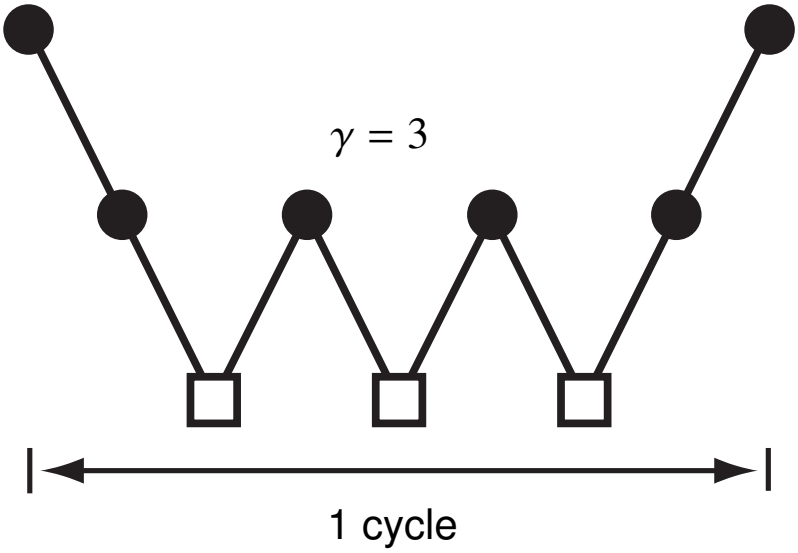

Fig. 2. Structure of W cycle with cycle index $\gamma = 3$ and three levels. Yokota_JOSAA_fig2.eps

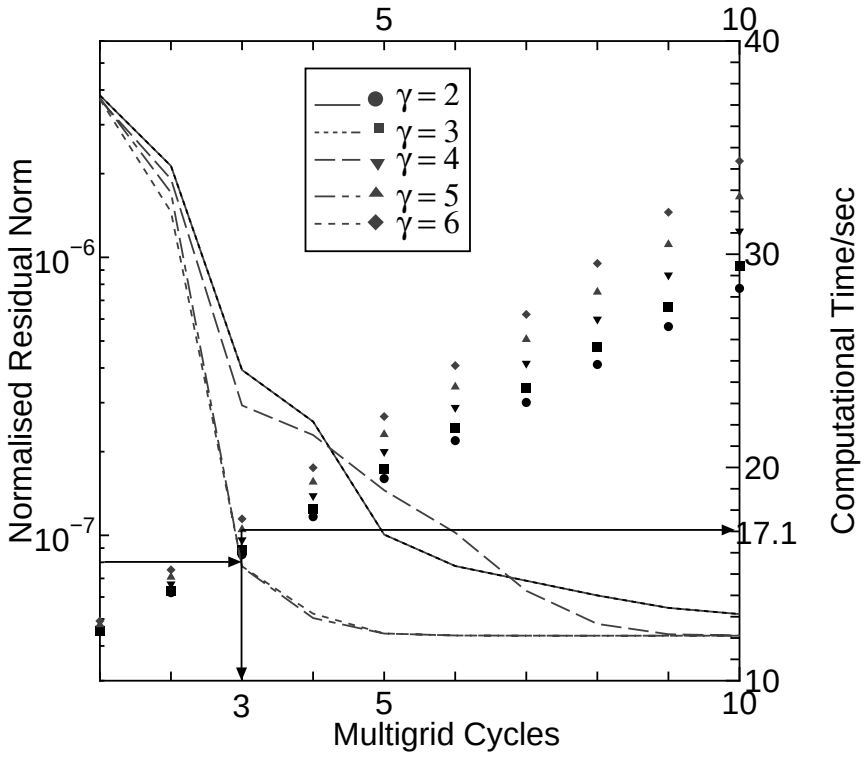

Fig. 3. Normalized residual norm and CPU time for several cycle indices. The number of unknowns $N = 8100$ and the matrix equation on the finest grid is solved under the condition that the normalized residual norm is less than 10^{-5}. Yokota_JOSAA_fig3.eps.

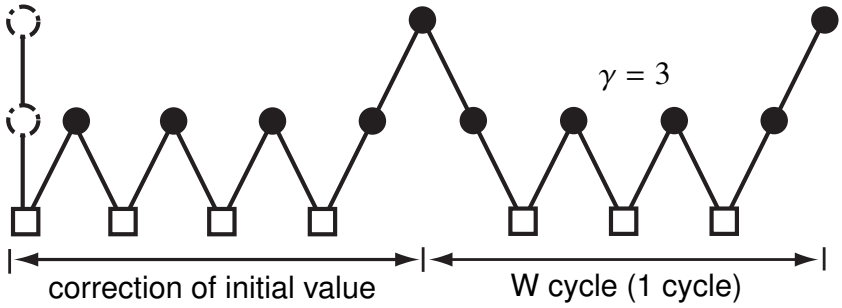

Fig. 4. Scheme for the improvement of the initial values for the multigrid. Yokota_JOSAA_fig4.eps

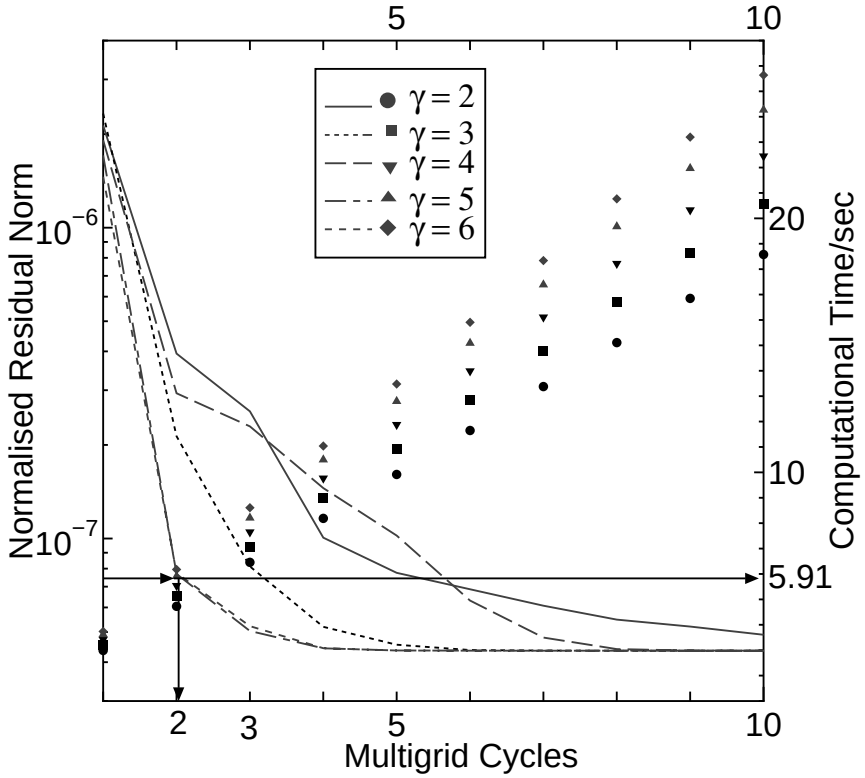

Fig. 5. Normalized residual norm and CPU time for several cycle indices using the scheme indicated in Fig. 4. Yokota_JOSAA_fig5.eps

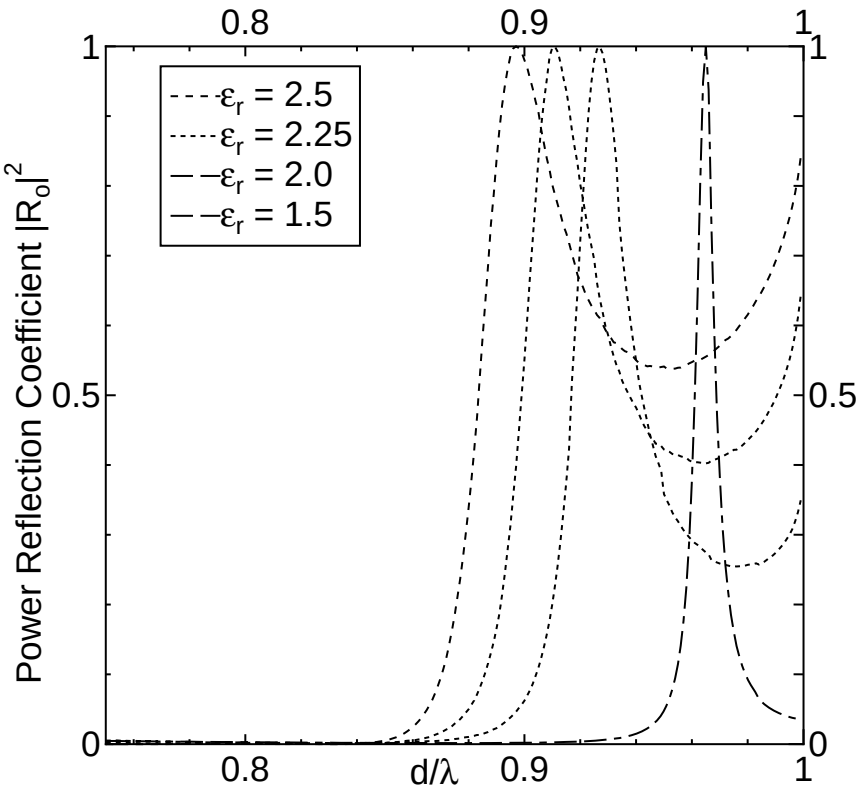

Fig. 6. Power reflection coefficient $|R_0|^2$ of the fundamental space harmonics for several different relative permittivity as function of the normalized frequency d/λ; radius of circular cylinder is $0.3d$. Yokota_JOSAA_fig6.eps.

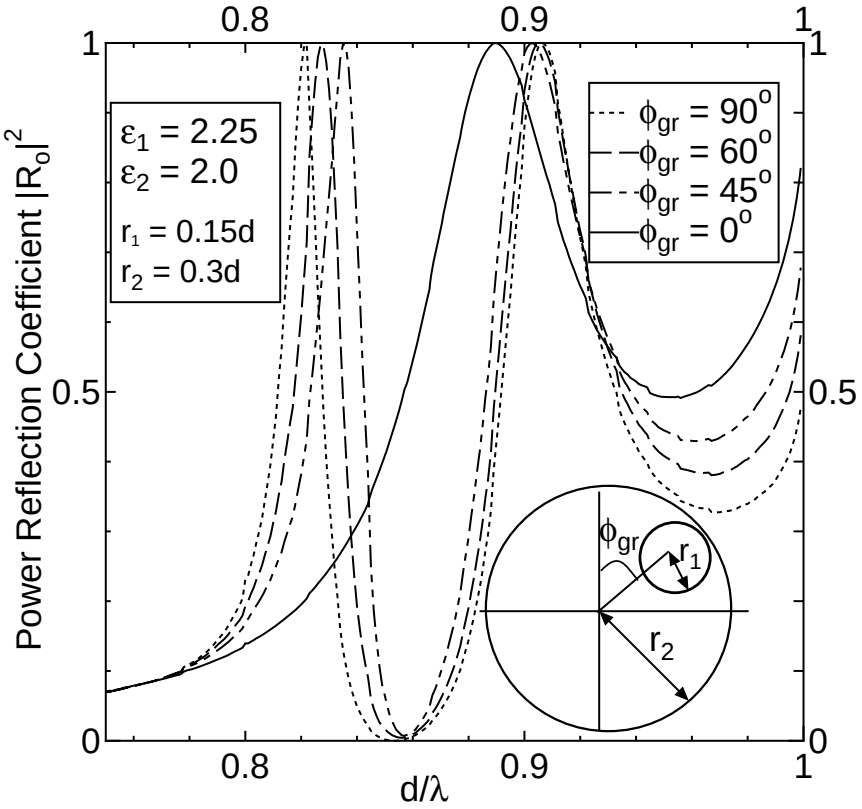

Fig. 7. Power reflection coefficient$|R_0|^2$ of the fundamental space harmonics for several different inclination angles Φ_{gr} as function of the normalized frequency d/λ; $\varepsilon_r = 2.25, \varepsilon_2 = 2.0, r_1 = 0.15d, r_2 = 0.3d$. Yokota_JOSAA_fig7.eps.

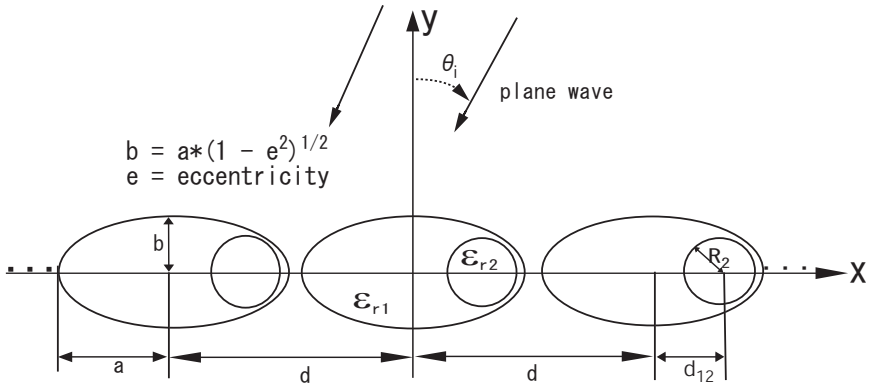

Fig. 8. Geometry of a periodic array of composite elliptical cylinders. Yokota_JOSAA_fig8.eps.

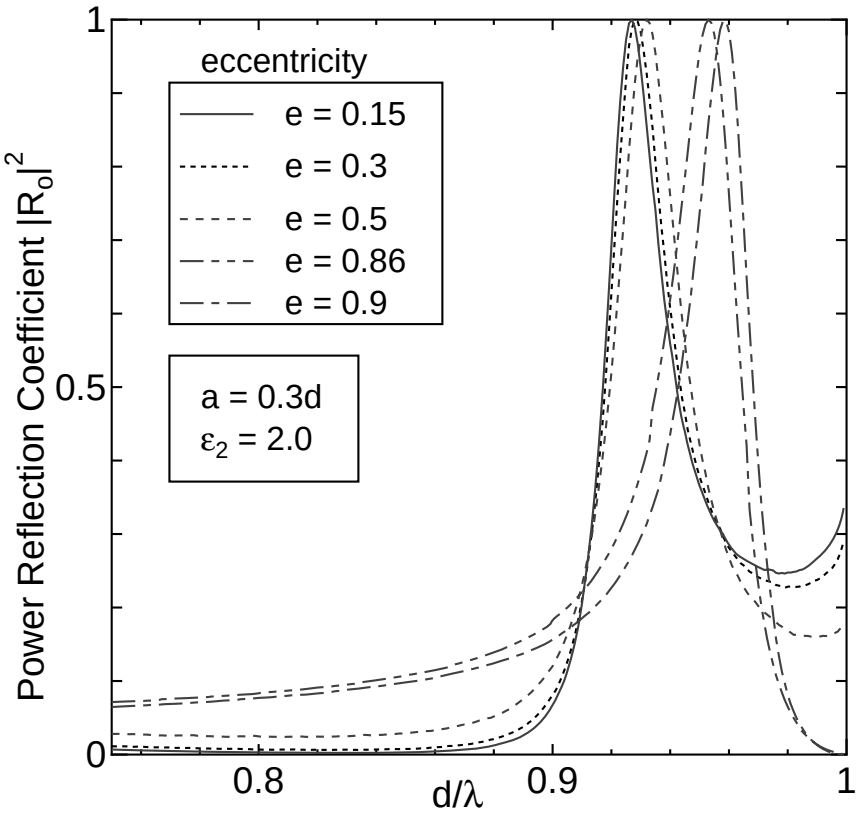

Fig. 9. Power reflection coefficient $|R_0|^2$ of the fundamental space harmonics for several different eccentricities as function of the normalized frequency d/λ; $a = 0.3d$ and $\varepsilon_2 = 2.0$. Yokota_JOSAA_fig9.eps

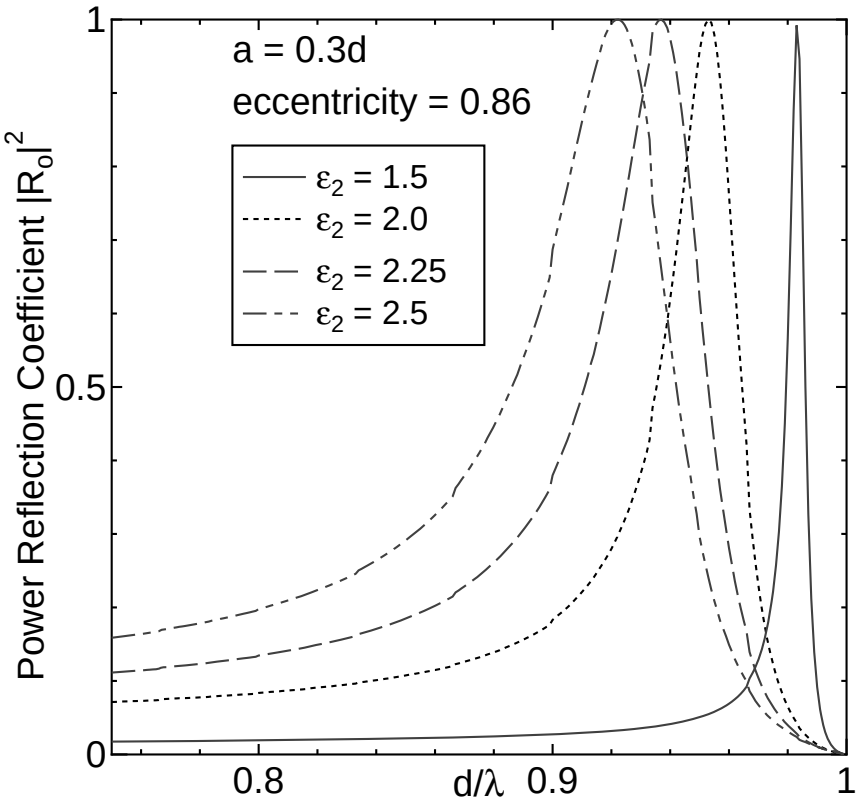

Fig. 10. Power reflection coefficient $|R_0|^2$ of the fundamental space harmonics for several different relative permittivity as function of the normalized frequency d/λ; $a = 0.3d$ and eccentricity is 0.86. Yokota_JOSAA_fig10.eps.

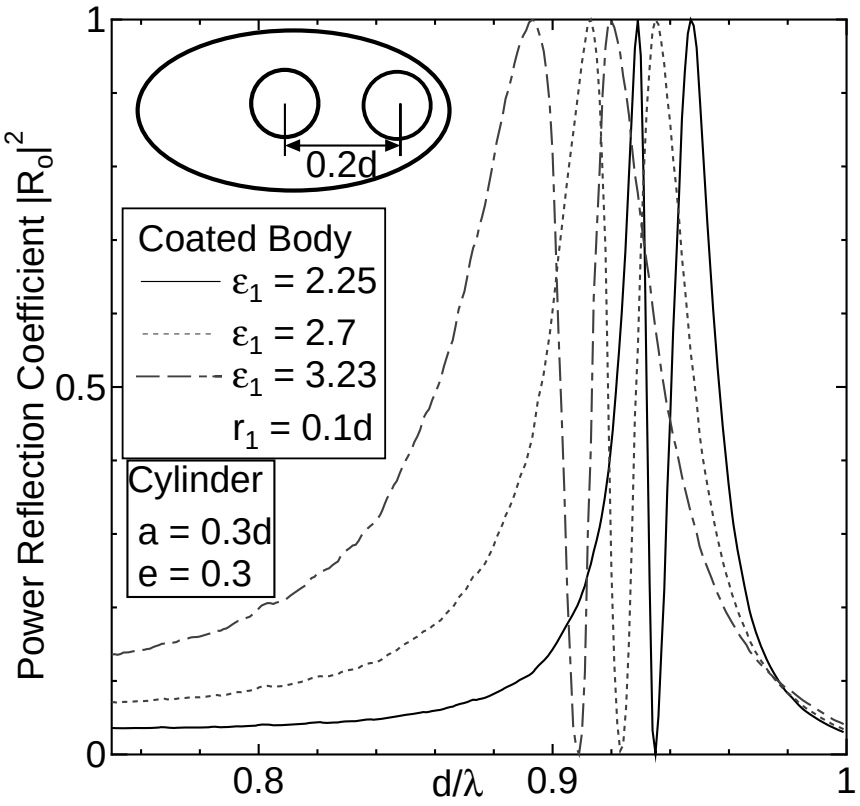

Fig. 11. Power reflection coefficient$|R_0|^2$ of the fundamental space harmonics for the elliptical cylinder where two circular cylinders are contained as function of the normalized frequency d/λ; $a = 0.3$ and eccentricity is 0.3. Yokota_JOSAA_fig11.eps.

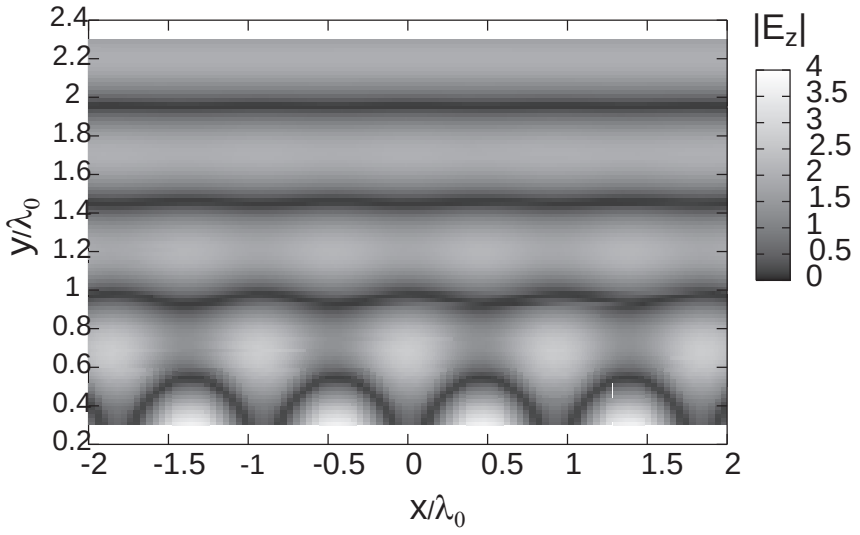

Fig. 12. Distribution of the total intensity contour distribution map; $d = 0.902\lambda$, $\varepsilon_{r1} = 3.23$, $R_1 = 0.1d$ and the eccentricity of the elliptical cylinder is 0.3 with $a = 0.3d$. Yokota_JOSAA_fig12.eps.